

A Power Conversion Model for Distributed PV Systems in California Using SolarAnywhere Irradiation

Mohammad Jamaly, Juan L Bosch, and Jan Kleissl

Dept. of Mechanical and Aerospace Eng., University of California, San Diego

March 15, 2013

Abstract

A high resolution 1 km satellite solar resource dataset (SolarAnywhere, SAW) was developed by Clean Power Research under the CSI program. A photovoltaic (PV) power conversion (or performance) model was generated to convert SAW irradiation to power output. The model was compared to measured power output from 192 PV systems over a year. The bias error between modeled and measured power output was found to be larger in summer (up to 5%) while SAW+performance model underestimate the measured data in the other months. A MATLAB version of the algorithm is provided at the CSI California Solar Research website.

1. Introduction

Clean Power Research's commercially available SolarAnywhere (SAW) provides Global Horizontal Irradiation (GHI) and Direct Normal Irradiation (DNI) derived from Geostationary Operational Environmental Satellite (GOES) visible imagery at 30 minutes temporal and 1 km spatial resolution [1]. To obtain GHI, a cloud index is calculated for each pixel from the reflectance measured by the satellite. Instantaneous, spatially averaged GHI is then calculated by using the cloud index along with a clear sky GHI model that considers local and seasonal effects of turbidity [2]. The instantaneous GHI is then converted to hourly irradiation assuming constant clear sky index (clear sky index is the ratio of actual irradiance versus that expected in clear sky conditions). DNI is obtained from clear-sky direct irradiance and GHI using the global-

to-DNI model, DIRINT, which is an evolution of NREL's DISC model, using a stability index derived from the consecutive records of GHI input [2].

Perez et al. [3] found an older version of the SAW algorithm to have mean bias errors (MBE) between -5 and 15 W m^{-2} and root mean square errors (RMSE, based on hourly averages) ranging from 73 - 118 W m^{-2} when compared against high quality ground measurements sites across the US. Jamaly et al. [4] validated SAW using ground measurements in 2010 at 52 California Irrigation Management Information System (CIMIS) stations and the NOAA Integrated Surface Irradiance Study (ISIS) network in Hanford, CA. SAW was unbiased compared to the Hanford ISIS data while SAW overestimated the measured GHI at CIMIS stations by $18.07 \pm 4.15 \text{ W m}^{-2}$ or $3.7\% \pm 0.9\%$ (95% confidence interval), on average. SAW was also biased large in clear conditions compared to GHI in clear sky conditions calculated based on the Ineichen model with Linke Turbidity from the SoDa database [2],[5],[6].

Jamaly et al. [7] also validated SAW using measured power output at 305 PV systems in California (in SDG&E, SCE, and PGE territories) in 2010. They applied the clear sky index (kt) to compare irradiation (SAW) and power (CSI) data. kt_{SAW} was found to overestimate kt_{CSI} by $3.80\% \pm 0.98\%$ (95% confidence interval) throughout the year. The biases were typically smaller during midday, but independent of month. Also, it was concluded that the main differences between kt_{SAW} & kt_{CSI} occurred in non-clear conditions (relative mean bias errors of 6.0%).

The objective of this study is to design and test a PV performance model that can be applied to SAW or other irradiances to accurately estimate power output at 305 PV systems in California for 2010. Section 2 covers the description of the datasets including their temporal interpolation, the performance model to convert the irradiance data into power, and error metrics. Results are presented in Section 3 and conclusions are made in Section 4.

2. Methodology

2.1. Datasets

The California Solar Initiative (CSI) rebate program requires a performance-based-incentive (PBI) payout for systems larger than 50 kW and makes it optional for smaller systems [8]. This requires metering and monthly submission of 15 minute energy output to the payout administrator. We have obtained the 2010 CSI measured output - quality controlled for system performance [9] - for 194, 385, and 403 PV power plants in San Diego Gas & Electric

(SDG&E), Southern California Edison (SCE), and Pacific Gas & Electric (PGE) territories (referred to as investor-owned utilities, IOUs) respectively.

The CSI database also includes street address and PV system specifications including DC Rating (kW_{DC}) at standard test condition (STC), AC Rating (kW_{AC}) at performance test condition (PTC), module and inverter models, inverter maximum efficiency, panel azimuth and tilt angles, and tracking type. The STC rating is obtained under idealized, controlled conditions of 1000 W m^{-2} plane-of-array irradiance and cell temperature at 25°C while the PTC is developed in an attempt to simulate more realistic conditions at 1000 W m^{-2} plane-of-array irradiance with panel temperature derived from ambient air temperature at 20°C and 1 m s^{-1} wind speed. Given the rapid increase in solar distributed generation (DG) in most coastal urban centers in California which are included in our study (e.g. Los Angeles, San Francisco, and San Diego) this dataset presents an important validation tool for PV power modeling research that could lead to more accurate solar forecasts for utilities and CAISO.

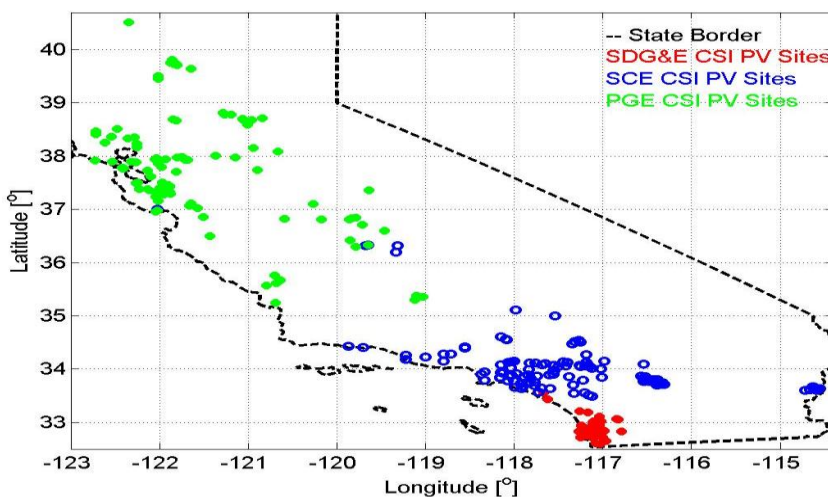


Fig. 1: Map of 192 PV systems in SDG&E, SCE, and PGE territories.

Quality control [10] was used to exclude all CSI sites with at least one of the following characteristics not representative of irradiance: PV systems with hourly averaged (versus 15 min) data, more than 70% missing data (mostly because they were installed during 2010), significant noise or large spikes in power due to recording issues, decrease in power due to soiling, significant clipping of power due to undersized inverters, system outages, systems with less than 5 distinct power outputs for the whole year, or plants divided into sub-arrays with different panel tilt and azimuth angles. Therefore, a final set of 192 PV systems are analyzed (Fig. 1 & Table 1).

To avoid errors due to sensor cosine response and shading by nearby obstructions (not considered by SAW), only data for solar zenith angles less than 75° are considered.

Table 1: Statistics of PV systems in SDG&E, SCE, and PGE territories

IOU	No. of PV systems	Total PTC rated capacity(MW)	Mean PTC rated (kW)	Median PTC rated (kW)
SDG&E	45	4.73	105.1	46.4
SCE	81	17.48	215.8	192.9
PGE	66	16.29	229.4	165.8

2.2. Performance Model

To convert SAW irradiation data for each site to CSI measured power output, a performance model has been developed. Using the GHI, DNI and tilt and azimuth angles of the PV panel, plane-of-array Global Irradiance (GI) is calculated using the Page model [11]. To predict cell temperature (T_{cell}) ambient air temperature and wind speed are obtained from measurements at the closest CIMIS station. Then, T_{cell} is calculated using a 1D transient heat transfer model [12], [13]. The temperature efficiency correction is then calculated as

$$\eta_{Temp} = 1 - \alpha(T_{cell} - 25^\circ \text{C}) \quad \text{Eq. (1),}$$

where α is the temperature coefficient and calculated such that the highest linear correlation between modeled and measured AC power output are obtained (see Appendix A). The DC power output of the PV system is estimated as

$$P_{SAW,DC} = kW_{DC} \cdot \eta_{Temp} \frac{GI}{1000 \text{ W m}^{-2}} \quad \text{Eq. (2).}$$

Inverter efficiency is modeled as [14]

$$\eta_{AC} = \frac{pf}{0.007 + 1.009 pf + (0.0975 pf)^2} \quad \text{Eq. (3),}$$

where the power factor is $pf = P_{SAW,DC} / kW_{AC}$.

Next maximum power point (MPP) efficiency is considered as [15]

$$\eta_{MPP} = a_1 + a_2 GI + a_3 \ln(GI) \quad \text{Eq. (4).}$$

The MPP efficiency is applied to correct typically observed deviations in modeled output from measurements across different irradiation values using empirically obtained coefficients a_1 , a_2 , and a_3 [16]. In this study, these coefficients are calculated such that the highest nonlinear

correlation between modeled and measured AC power output are obtained (see Appendix A). Then, the AC power output of the PV system is estimated as

$$P_{SAW,AC} = \eta_{AC} \cdot \eta_{MPP} \cdot P_{SAW,DC} \cdot C_f \quad \text{Eq. (5).}$$

where $C_f = \text{avg}(P_{CSI})/\text{avg}(P_{SAW,AC})$ accounts for the line losses and soiling by calibrating the modeled performance by the ratio of the annual average CSI measured to modeled power output. The calibration guarantees that modeled averaged annual performance based on SAW irradiation is consistent (or without bias) with observed performance. Such a ‘modeled output statistics’ (MOS) correction would typically also be applied in operational forecasting of PV power output.

According to Eqs. (1-5), the total solar irradiance to power conversion efficiency (η_{Tot}) is equal to

$$\eta_{Tot} = \eta_{Temp} \cdot \eta_{AC} \cdot \eta_{MPP} \cdot C_f \quad \text{Eq. (6).}$$

2.3. Temporal Matching between CSI and SAW data

SolarAnywhere provides 30-min average centered irradiation at :00 and :30. CSI provides 15-min averaged power output with an interval-ending timestamp at :00, :15, :30, and :45. Consequently, two CSI intervals are aggregated to compare against the corresponding SAW interval.

2.4. Error Metrics

Mean Bias Error (MBE) describes persistent differences between $P_{SAW,AC}$ and P_{CSI} . Mean Absolute Error (MAE) and Root Mean Square Error (RMSE) describe random differences between $P_{SAW,AC}$ and P_{CSI} . MBE, MAE, and RMSE are calculated as

$$\left\{ \begin{array}{l} MBE = \frac{1}{N} \sum_{n=1}^N (P_{SAW,AC} - P_{CSI}) \\ MAE = \frac{1}{N} \sum_{n=1}^N \text{abs}(P_{SAW,AC} - P_{CSI}) \\ RMSE = \frac{1}{N} \sqrt{\sum_{n=1}^N (P_{SAW,AC} - P_{CSI})^2} \end{array} \right. \quad \text{Eq. (7),}$$

where N is the number of samples. Also, the relative MBE (rMBE), relative MAE (rMAE), and normalized RMSE (nRMSE) are calculated as

$$\begin{cases} rMBE = \frac{MBE}{\text{mean}(P_{CSI})} * 100\% \\ rMAE = \frac{MAE}{\text{mean}(P_{CSI})} * 100\% \\ nRMSE = \frac{RMSE}{\text{mean}(P_{CSI})} * 100\% \end{cases} \quad \text{Eq. (8).}$$

To illustrate diurnal or seasonal patterns in the data, bias errors are averaged for each time of day (ToD) and each month separately to yield MBE_{MT} [17] as the difference between $P_{SAW,AC}^*(m, ToD)$ and $P_{CSI}(m, ToD)$ for $m = 1, \dots, 12$ (months) and $ToD = 1, \dots, 48$ (30 min segments).

$$rMBE_{MT}(m, ToD) = \frac{MBE_{MT}(m, ToD)}{\text{mean}[P_{CSI}(m, ToD)]} * 100\% \quad \text{Eq. (9).}$$

3. Results

3.1. Comparison of California-wide modeled power output averages across the year

$P_{SAW,AC}$ and P_{CSI} averaged for the SDG&E, SCE, and PGE territories along with the overall average for all three IOUs together are computed for the year 2010 (Fig. 2). Since the results do not differ significantly by IOU, for the remainder of the report, only averages across all three IOUs are shown. The average SAW and CSI power outputs are in good agreement for all three IOUs: They are essentially unbiased on average due to the calibration (C_f in Eq. 5) with small random errors. Typical differences (as measured by the rMAE and nRMSE) between the calibrated modeled and measured performance are 4 to 9% for 30-min averaged data.

The average calibration factor of 0.91, C_f in Eq. 5, confirms that the performance model generally overestimates before calibration, likely since line losses and soiling of the PV systems that are not considered.

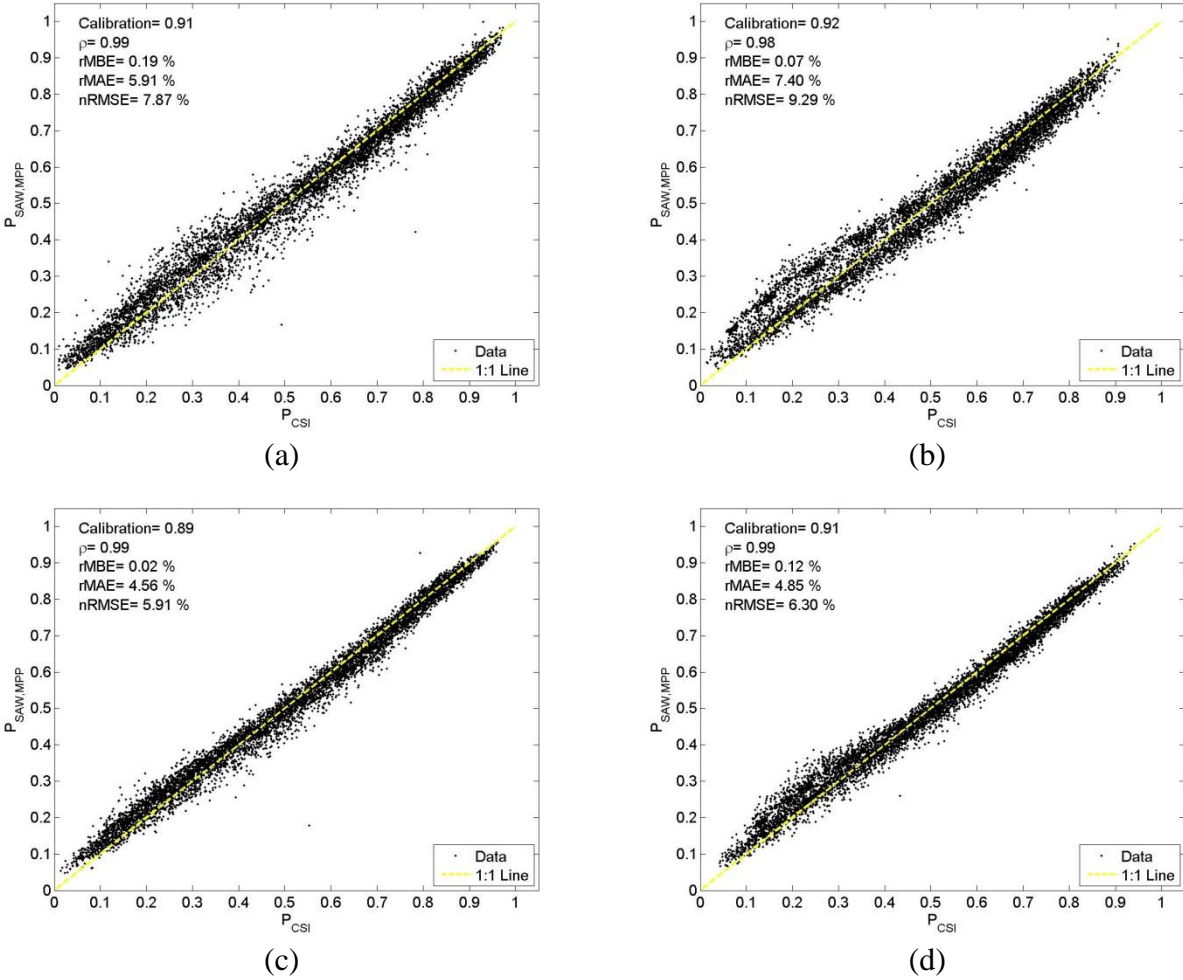


Fig. 2: Modeled SolarAnywhere versus measured power output: 30 min power output (for $SZA < 75^\circ$) in 2010 averaged over (a) SDG&E (45 PV sites), (b) SCE (81 PV sites), (c) PGE (66 PV sites), and (d) combined. The caption indicates the calibration factor (Eq. 5), the correlation coefficient (ρ), rMBE, rMAE, nRMSE between $P_{SAW,AC}$ and P_{CSI} .

The average temperature coefficient (used in Eq. 1) was found to be $\alpha = 5.5 \times 10^{-3} \text{ K}^{-1}$. Figure 3 shows histogram of the temperature coefficient for all PV systems. Temperature coefficients are expected to be between $3 \times 10^{-3} \text{ K}^{-1}$ for thin film and $5 \times 10^{-3} \text{ K}^{-1}$ for silicon solar cells. Since mounting details of individual PV systems was unknown the spread in temperature coefficients is also due to inaccuracies in the temperature model. Especially the spacing of the panel from the roof and roof properties can significantly affect convection heat losses and heat gain due to radiative interactions.

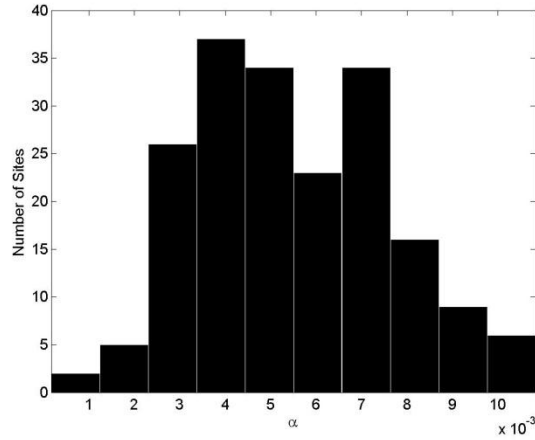


Fig. 3: **Histogram of temperature coefficient (α)** for all 192 PV sites.

The daily and monthly average PV solar conversion efficiency (η_{Tot}), average over all the PV sites, is shown in Fig. 4. The annual average η_{Tot} is 78.5%. The histogram of annual average of η_{Tot} for all PV systems is presented in Fig. 5. Note that η_{Tot} is not the solar conversion efficiency that would be reported on a specification sheet of a solar module or even the plant solar conversion efficiency. Rather, since the panel area is unknown, only relative real-world efficiencies considering losses due to (likely in this order) temperature, line, soiling, and inverters can be considered. The trends in Fig. 4 are dominated by lower temperatures and consequently higher efficiencies during the winter.

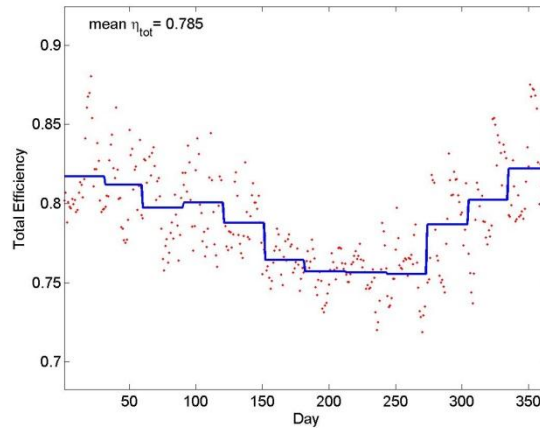


Fig. 4: **Daily average relative solar conversion efficiency (SCE, η_{Tot})** averaged over 192 PV sites. The blue line represents monthly averages and the caption shows the annual average of η_{Tot} , averaged over 192 PV sites.

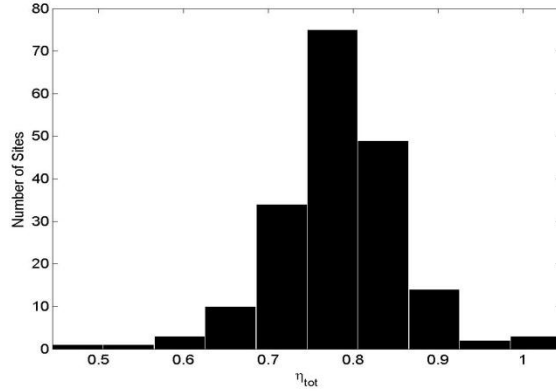


Fig. 5: **Histogram of relative PV solar conversion efficiency (η_{Tot})** for all 192 PV sites.

Dependencies of the error in modeled performance on cell temperature, ambient temperature, wind speed, zenith angle, and inverter efficiency were examined. However, no trend in the error was found (not shown) indicating that a more complex model for these variables would not necessarily improve the agreement. The remaining random errors (RMSE) could be related to the temperature model and stem from the irradiation input data due to location errors in the SAW cloud fields (satellite navigation errors and cloud-to-shadow parallax).

3.2. Climatologies of MBE by month and time-of-day

Averaged $rMBE_{MT}$ of all PV systems is shown in Fig. 7. Generally, the biases are less than 3% during midday. $P_{SAW,AC}$ underestimates P_{CSI} especially in March through May mornings, while $P_{SAW,AC}$ overestimates for small SZAs.

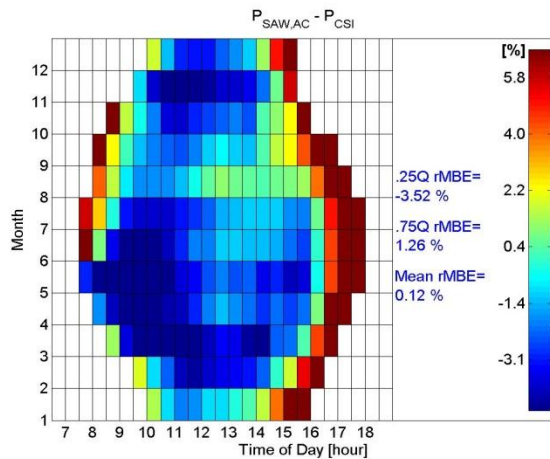


Fig. 7, **rMBE by month and time-of-day for $P_{SAW,AC}$ versus P_{CSI}** (averaged over 192 PV sites) in 2010. The caption indicates mean, 0.25 and 0.75 quantiles of rMBE.

3.3. Comparison to PVWATTS

PVWATTS is a standard calculator of PV performance maintained by NREL. For three representative sites, the PVWATTS PV performance was computed by Stephan Barsun (Itron) and compared to our performance model (Table 2).

Generally PVWATTS and our model provide similar results. Our model performs slightly better, but the bias was calibrated to be zero in our model which probably also explains some of the improvement in MAE and RMSE. While the performance is not significantly better, one of the big advantages of our MATLAB model is the ‘true up’ to a significant amount of real metered data as opposed to the defaults in PVWATTS and ability to use different time steps.

Table 2: Relative Mean Bias Error (rMBE) and relative mean absolute error (rMAE) for three different CSI PV sites in California. The following datasets are compared: PVWATTS (PVW), the performance model described in this chapter (us), and the measured CSI data.

Error Metric	Site 1	PVW - Us - CSI	Site 2	PVW - Us - CSI	Site 3	PVW - Us - CSI
	PVW-us CSI		PVW-us CSI		PVW-us CSI	
rMBE [%]	-1.6	-2.15	-2.4	-2.9	-4.4	-4.8
rMAE [%]	3.7	9.8	1.3	7.9	4.5	9.5

As an aside, PowerClerk now tracks PV module mounting by standoff which will facilitate more accurate PV temperature modeling due to variation of convection losses on the back side of the module. In particular, standoffs are classified into, flush, 0 to 1, 1 to 3, and 3 to 6 inches.

4. Conclusions

A PV performance model was developed to calculate the expected power output for each PV system from SolarAnywhere (SAW) irradiation data (hereinafter referred to as SAW+P). Modeled power output was validated against measured power output from 192 PV systems in California (in SDG&E, SCE, and PGE territories) in 2010. An average PV efficiency derate (η_{Tot}) of 79% (loss of 21%) describes losses due to panel temperature, AC conversion, MPP tracking, and annual calibration. The average calibration factor of 0.91 confirms that the SAW+P model generally overestimates, likely due to line losses and soiling of the PV systems that are not considered in Eq. 5. The bias error between modeled and measured power output was found to be less than 3% during middays while SAW+P underestimates the measured data in winter and spring times. SAW+P provides a validated means to simulate real world system

performance and integrate PV simulations into grid simulations or other tools. SAW+P does not, however, account for losses due to complete system outages due to maintenance, etc.

A MATLAB version of the algorithm is provided at the CSI California Solar Research website.

5. References

1. Web-based Clean Power Research service database, SolarAnywhere. Available: <https://www.solaranywhere.com/Public/About.aspx>
2. Perez, R., Ineichen, P., Moore, K., Kmiecik, M., Chain, C., George, R., and Vignola, F., "A new operational model for satellite-derived irradiances: Description and validation," *Solar Energy*, 73(5):307-317, 2002.
3. Perez, R., Kivalov, S., Schlemmer, J., Hemker, K., Renné, D., and Hoff, T., "Validation of short and medium term operational solar radiation forecasts in the US," *Solar Energy*, 84(12):2161-2172, 2010.
4. M. Jamaly and J. Kleissl, Validation of SolarAnywhere Enhanced Resolution Irradiation in California, Internal Report, 2012.
5. P. Ineichen, "Comparison of eight clear sky broadband models against 16 independent data banks," *Solar Energy*, 80:468-478, 2006.
6. Solar Radiation Database (SoDa). Available: <http://www.soda-is.com>
7. M. Jamaly, J.L. Bosch, and J. Kleissl, Validation of SolarAnywhere Enhanced Resolution Irradiation Using Power Output of Distributed PV Systems in California, Internal Report, 2012.
8. California Solar Initiative, "California Public Utilities Commission California Solar Initiative Program Handbook," Accessed Sep. 2011 at: http://www.gosolarcalifornia.org/documents/CSI_HANDBOOK.PDF
9. Itron, Inc. & KEMA, Inc., "CPUC California Solar Initiative 2009 Impact Evaluation," Jun. 2010. Available: http://www.cpuc.ca.gov/NR/rdonlyres/70B3F447-ADF5-48D3-8DF0-5DCE0E9DD09E/0/2009_CSI_Impact_Report.pdf
10. J. Luoma and J. Kleissl, Summary of Quality Control for 2010 CSI Data, Internal Report, 2012.
11. J. Page, "The Role of Solar Radiation Climatology in the Design of Photovoltaic Systems," in: T. Markvart, L. Castaner, *Practical Handbook of Photovoltaics: Fundamentals and Applications*, Elsevier, Oxford, 2003, pp. 5-66.
12. M.W. Davis, A.H. Fannery, and B.P. Dougherty, "Prediction of Building Integrated Photovoltaic Cell Temperatures," *Transactions of the ASME*, V.123: 200-210, 2001.
13. A.D. Jones and C.P. Underwood, "A Thermal Model for Photovoltaic Systems," *Solar Energy* Vol. 70, No. 4, pp. 349-359, 2001.
14. J. Luoma, J. Kleissl, and K. Murray, "Optimal Inverter Sizing Considering Cloud Enhancement," *Solar Energy*, 86(1): 421-429, 2012.
15. S.R. Williams, T.R. Betts, T. Helf, R. Gottschalg, H.G. Beyer, and D.G. Infield, "Modelling Long-Term Module Performance based on Realistic Reporting Conditions with Consideration to Spectral Effects," 3rd World Conference on Photovoltaic Energy Conversion, Osaka, Japan, May 11-18, 2003.
16. H.G. Beyer, J. Betcke, A. Drews, D. Heinemann, E. Lorenz, G. Heilscher, and S. Bofinger, S, "Identification of a General Model for the MPP Performance of PV-Modules for the Application in a Procedure for the Performance Check of Grid Connected Systems," 19th European Photovoltaic Solar Energy Conference and Exhibition, Paris, France, 07.06.-11.6.2004, pp3073-3076.
17. A. Nottrott and J. Kleissl, "Validation of the NSRDB-SUNY global horizontal irradiance in California," *Solar Energy*, 84(10):1816-1827, 2010.

Appendix A: Procedure to Calculate Temperature and MPP Efficiencies

For each PV system, the temperature (linear regression) and MPP (nonlinear regression) efficiencies are calculated such that the highest correlation between modeled and measured AC power output are obtained (in 2 steps).

First, $P_{SAW,DC,i}$ and, then, $\eta_{AC,i}$ are calculated using Eqs. 2-3 by assuming the temperature coefficient (α in Eq. 1) $\alpha = 5 \times 10^{-3} \text{ K}^{-1}$ (this is a widely used value for α for silicon PV which is applied as an initial guess). The initial performance AC output is

$$P_{SAW,AC,i} = \frac{kW_{DC} \cdot GI}{1000 \text{ Wm}^{-2}} \cdot \left[1 - 0.005 \text{ K}^{-1} (T_{cell} - 25^\circ \text{C}) \right] \eta_{AC,i} \cdot \left[a_{1,i} + a_{2,i} \cdot GI + a_{3,i} \cdot \ln(GI) \right] \quad \text{Eq. (A1)},$$

where $P_{SAW,AC,i}$ is an initial guess for AC performance output. The initial guess for MPP efficiencies $a_{1,i}$, $a_{2,i}$, and $a_{3,i}$ are obtained using nonlinear fit between $P_{SAW,AC,i}$ and P_{CSI} .

Then, by applying the obtained values for the initial MPP efficiencies $a_{1,i}$, $a_{2,i}$, and $a_{3,i}$, the performance AC output at the second step is

$$P_{SAW,AC,i2} = kW_{DC} \cdot \frac{GI}{1000 \text{ Wm}^{-2}} \cdot \left[1 - \alpha (T_{cell} - 25^\circ \text{C}) \right] \eta_{AC,i} \cdot \eta_{MPP,i} \quad \text{Eq. (A2)},$$

where $\eta_{MPP,i} = a_{1,i} + a_{2,i} \cdot GI + a_{3,i} \cdot \ln(GI)$. α is obtained using linear correlation between $P_{SAW,AC,i2}$ and P_{CSI} .

Afterwards, by applying the obtained temperature coefficient (α), the temperature efficiency, DC power output, inverter efficiency, MPP efficiency, and AC power output are calculated using Eqs. 1-5. Note that the calibration factor (C_f in Eq. 5) is essentially the product of the constant coefficients in the two correlation steps above.

To observe how well the efficiency coefficients fitted, temperature, inverter, and MPP efficiencies are calculated based on the P_{CSI} as $P_{CSI} \cdot 1000 \text{ Wm}^{-2} / (kW_{DC} \cdot \eta_{AC} \cdot \eta_{MPP} \cdot C_f)$, $P_{CSI} \cdot 1000 \text{ Wm}^{-2} / (kW_{DC} \cdot \eta_{Temp} \cdot \eta_{MPP} \cdot C_f)$, and $P_{CSI} \cdot 1000 \text{ Wm}^{-2} / (kW_{DC} \cdot \eta_{Temp} \cdot \eta_{AC} \cdot C_f)$ respectively (These are called measured efficiencies hereafter). Measured η_{Temp} against T_{cell} , measured η_{AC} against power factor (pf), and measured η_{MPP} against GI are shown in Figs. A1-A3 respectively. These plots are shown for a representative PV site (site # SD-CSI-00618) and averaged over all the PV sites as well. Fig. A1 shows fitted line where the slope of this line is the temperature coefficient which is obtained in this study.

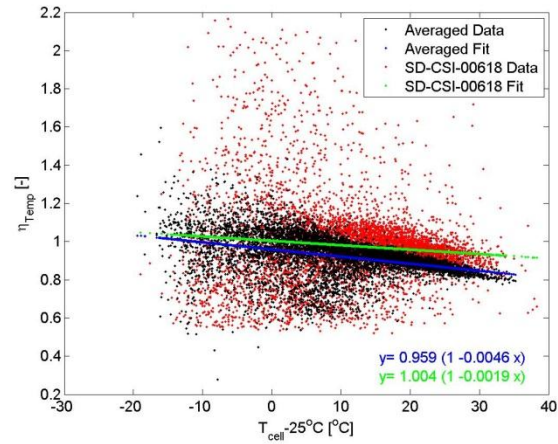


Fig. A1: Measured temperature efficiency (η_{Temp}) versus T_{cell} for SD-CSI-00618 PV system (red) and averaged over all the PV sites (black).

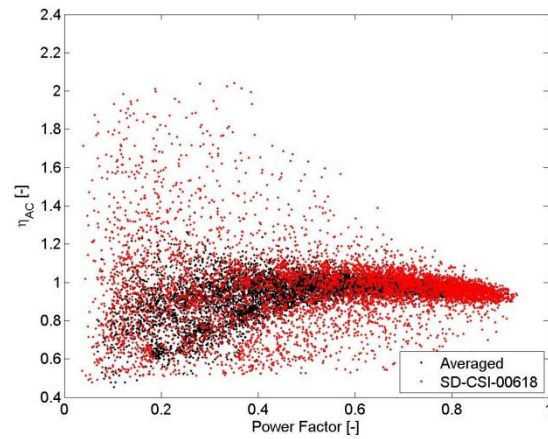


Fig. A2: Measured inverter efficiency (η_{AC}) versus power factor (Pf) for SD-CSI-00618 PV system (red) and averaged over all the PV sites (black).

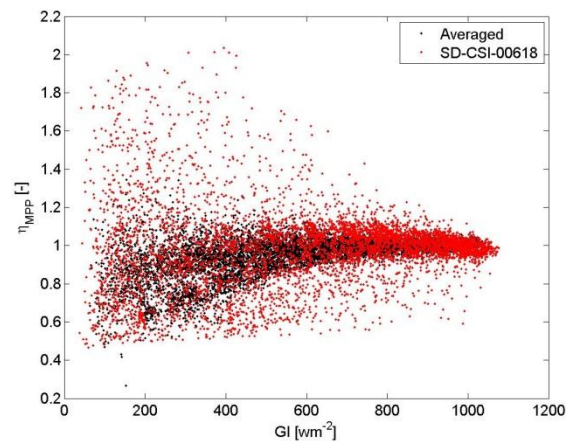


Fig. A3: Measured MPP efficiency (η_{MPP}) versus GI for SD-CSI-00618 PV system (red) and averaged over all the PV sites (black).

To illustrate the effects of different submodels of the PV performance model, the power performance submodels are added in step-by-step:

$$\begin{cases} P_{SAW,r} = kW_{DC} \cdot \frac{GI}{1000 \text{ Wm}^{-2}} \\ P_{SAW,DC} = \eta_{Temp} \cdot P_{SAW,r} \\ P_{SAW,AC1} = \eta_{AC} \cdot P_{SAW,DC} \cdot C_f \\ P_{SAW,AC} = \eta_{MPP} \cdot P_{SAW,AC1} \end{cases} \quad \text{Eq. (A3).}$$

$P_{SAW,r}$, $P_{SAW,DC}$, and $P_{SAW,AC1}$ against P_{CSI} averaged over all the PV sites are shown in Figs. A4-A6 respectively (averaged $P_{SAW,AC}$ against P_{CSI} for all the PV sites is shown in Fig. 2d). Note that $P_{SAW,r}$ and $P_{SAW,DC}$ are normalized by DC rated capacity while P_{CSI} , $P_{SAW,AC1}$, and $P_{SAW,AC}$ are normalized by CSI (based on CEC PTC) rated capacity of all the PV systems.

Fig. A4 confirms the fact that the performance model overestimates power output if no efficiency and loss coefficients are applied. The DC performance output needs to be modified according to temperature efficiency (Fig. A5). Fig. 6 shows the AC output by applying the inverter efficiency. However, the performance model overestimates at lower irradiances while it underestimates at higher irradiances, which is relaxed by applying MPP efficiency (Fig. 2d). Based on the correlation method applied in this study, a calibration factor of 0.89 is obtained which mostly accounts for the line losses and soiling (usually a 0.9 coefficient is considered for such losses).

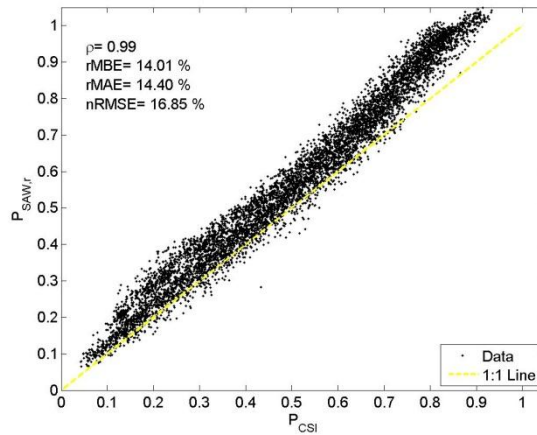


Fig. A4: Similar to Fig. 2d but for $P_{SAW,r}$ versus P_{CSI} .

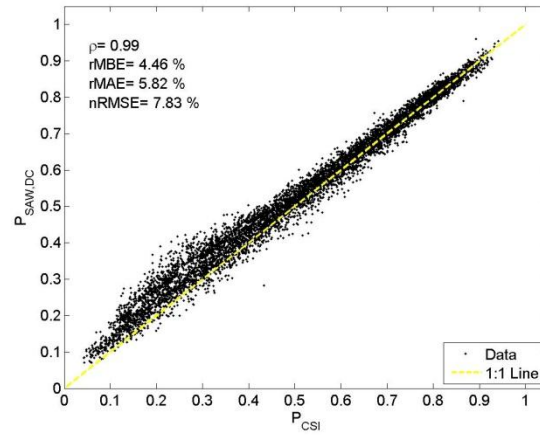


Fig. A5: Similar to Fig. 2d but for $P_{SAW,DC}$ versus P_{CSI} .

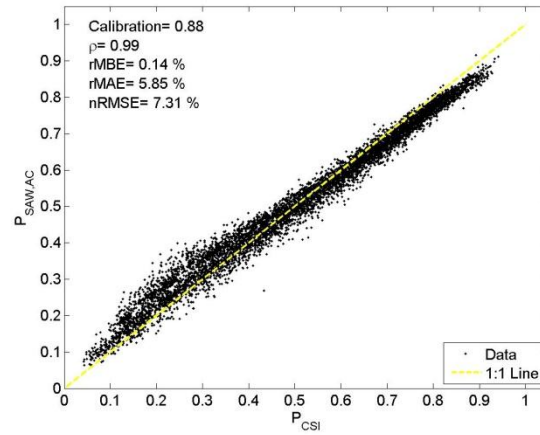


Fig. A6: Similar to Fig. 2d but for $P_{SAW,ACI}$ versus P_{CSI} .